Locating fluorescence lifetimes behind turbid layers non-invasively using sparse, time-resolved inversion

Guy Satat[1], Christopher Barsi*[1], Barmak Heshmat[1], Dan Raviv[1], and Ramesh Raskar[1]
Media Lab, Massachusetts Institute of Technology, 77 Massachusetts Ave., Cambridge, MA 02139, USA
**cbarsi@mit.edu*

Abstract: We use time-resolved sensing and sparsity-based dictionary learning to recover the locations and lifetimes of fluorescent tags hidden behind a turbid layer. We experimentally demonstrate non-invasive target classification via fluorescence lifetimes.
OCIS codes: (280.1350) Backscattering; (110.0113) Imaging through turbid media; (320.7100) Ultrafast measurements.

1. Introduction

Imaging through scattering media is a pervasive problem in optics, as scattering precludes direct image formation. A recent time-resolved method utilized the time profile of scattered light for reconstructing three-dimensional (3D) shapes that were hidden from view [1]. However, determining the presence or absence of an object, among a finite number of possibilities, is often sufficient for remote sensing applications. This suggests the use of fluorescent markers as identifiers. Fluorescence has already been used in remote sensing [2], but ambiguous spectra can cause errors in reconstruction. Therefore, we rely on the lifetime of the fluorescence emission to separate different samples. Here, we non-invasively illuminate fluorescent samples and record the time-resolved light scattered by a turbid layer. We reconstruct the locations and lifetimes, τ, of each sample using a sparsity-based metric.

2. Method

Figure 1 (a) shows the optical setup. A Ti-Sapph. laser (*795* nm, *75* MHz repitition rate, and *50* fs pulse duration) is frequency-doubled to ~ *400* nm and is then focused onto a polycarbonate diffuser (Edmund Optics, 55-444) with a scattering angle of *60°*. Light is scattered toward three 1.5×1.5 cm^2 square patches located behind the diffuser. The first patch is non-fluorescing (NF), cut from a white MacBeth Colorchecker square. The second patch is painted with a CdSe–CdS quantum dot solution ($\tau = 32$ ns) (QD) [3]. The third patch is painted with pyranine ink ($\tau = 5$ ns) (PI). Light is scattered from these samples back toward the diffuser, the front side of which is imaged onto a streak camera with a time resolution of ~ *2* ps. To study the time-resolved scattering of both the *400* nm excitation and the fluorescent emission, images are recorded both with and without a UV cutoff filter ($\lambda_{cut} = 450$ nm). A pair of galvo mirrors scans the incident laser through *12* different points, and a streak image is recorded for each one. Experimental measurements are shown in Figure 2 (left).

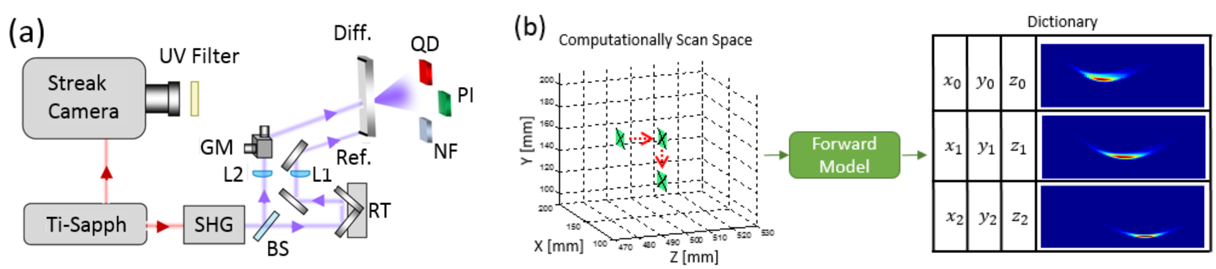

Fig. 1. (a) Optical Setup. A Ti-Sapph. laser is frequency-doubled and split via a beam splitter (BS). One path is used as a reference on the diffuser, using a retro-reflector (RT) for a delay line. The second path is controlled by two galvo mirrors (GM) and focused onto the diffuser. Behind the diffuser are three patches: quantum dot (QD), pyranine ink (PI), and a non-fluorescing patch (NF). (b) Dictionary generation schematic: a patch is computationally moved in space. Forward modeling generates a streak image that is stored with the patch's *X*, *Y*, *Z* location.

To make the algorithm more robust, we first reconstruct the patch geometry, and recover the lifetimes subsequently (Fig. 2). To recover geometry, we first learn a dictionary offline by computationally scanning the volume space with a single patch and computing the expected streak image via the time-resolved forward model, ignoring fluorescence. Each atom of the resulting dictionary (Fig. 1b) comprises the intensity values of all 12 illumination points. The reconstruction is effected with orthogonal matching pursuit (OMP) [4] to discover which dictionary atoms are best correlated with the measured streak images:

$$\min_x \ \|x\|_0 \quad subject\ to \quad Dx = y\,, \qquad (1)$$

where x is the selected atoms vector, $||x||_0$ is the sparse norm (counting number of non-zero elements), D is the dictionary matrix, and y is the measurements vector (*12* illumination points, stacked to a vector). The location of the atom in the dictionary yields the patch location in the physical volume. With these optimized patch locations, we convolve the resulting (reconstructed) streak images with all possible fluorescence lifetime decay responses and choose the lifetimes that best agree with the observations.

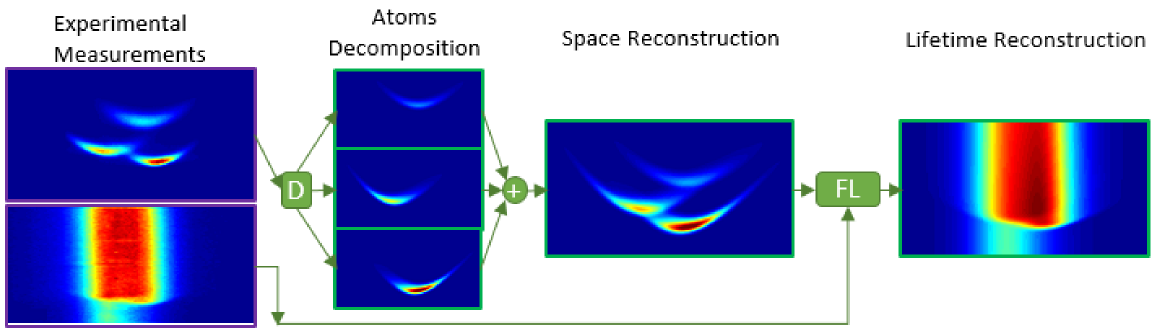

Fig. 2. Reconstruction flow. Left: input streak images (top, without UV filter; bottom, with UV filter). The top image is decomposed into atoms via dictionary D (center left) with OMP, thus reconstructing positions X, Y, and Z for all patches (center right). The reconstructed locations are used next to generate all possible fluorescence options, and the best match with data is selected to distinguish patches via lifetimes (right).

3. Results

We succusfully reconstructed multiple patch configurations, and a sample result is shown in Fig 3. Fig. 3 (a) shows a photograph of the scene: three patches on the right and the diffuser on the left. The camera and illumination (not shown) are both to the left of the diffuser. The PI ($\lambda_{reflect} \sim 510$ nm), QD ($\lambda_{reflect} \sim 600$ nm), and NF ($\lambda_{reflect} \sim 400$ nm) patches are located, respectively, from the background to the foreground. Fig. 3(b) shows the geometry reconstruction for all three patches, with the quantitative results in Fig. 3(c). Our method here successfully reconstructs the geometry to within *1* cm, which is typical resolution requirements for remote sensing and deep tissue imaging applications. Finally, because we assume only a finite number of lifetimes, the algorithm distinguishes between the PI, the QD, and the NF patches with *100%* accuracy.

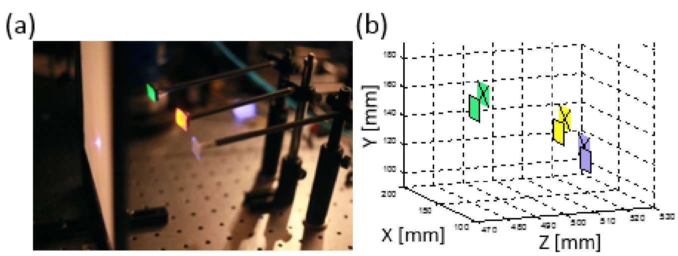

(c)

Reconstruction Error

Patch	ΔX [mm]	ΔY [mm]	ΔZ [mm]	$\Delta \tau$
Non-fluorescing	7.74	7.54	1.27	0
Quantum dot	9.87	1.20	1.61	0
Phospurous ink	10.86	5.66	1.66	0

Fig. 3. Reconstruction results. (a) Experimental setup. (b) Geometry and lifetime reconstruction with ground truth. Green, yellow, and purple correspond to NF, QD, and PI patches, respectively. Patches with an 'X' are the reconstructed locations, with the solid outline corresponding to ground truth. (c) Reconstruction error for the three patches. The dictionary space has resolution dx = 6.9 mm, dy = 7.5 mm, dz = 5.2 mm.

4. Conclusions

We demonstrated the time-resolved inversion of scattered light to locate fluorescent tags behind turbid layers and distinguish their lifetimes, based on spatial sparsity. This has potential applications in remote sensing of spectrally identical fluorescent tags, as well as potential algorithmic benefits for fluorescence lifetime tomography.

5. References

[1] A. Velten, T. Willwacher, O. Gupta, A. Veeraraghavan, M. G. Bawendi, and R. Raskar, "Recovering three-dimensional shape around a corner using ultrafast time-of-flight imaging," Nat. Commun. 3, 745 (2012).

[2] F. E. Hoge and R. N. Swift, "Airborne simultaneous spectroscopic detection of laser-induced water Raman backscatter and fluorescence from chlorophyll a and other naturally occurring pigment," Appl. Opt. 20, 3197-3205 (1981).

[3] O. Chen, J. Zhao, V. P. Chauhan, J. Cui, C. Wong, D. K. Harris, H. Wei, H.-S. Han, D. Fukumura, R. K. Jain, and M. G. Bawendi, "Compact high-quality CdSe–CdS core–shell nanocrystals with narrow emission linewidths and suppressed blinking," Nat. Mat. 12, 445-451 (2013).

[4] D. L. Donoho, M. Elad, and V. N. Temlyakov, "Stable recovery of sparse overcomplete representations in the presence of noise," IEEE Trans. Information Theory 52, 6-18 (2006).